Transition between an exothermic chemical wave front and a generic flame

G. Dumazer,[1] M. Leda,[1,2] B. Nowakowski,[2,3] and A. Lemarchand[1,*]

[1]*CNRS, Laboratoire de Physique Théorique de la Matière Condensée, Université Pierre et Marie Curie, UMR 7600, 4 place Jussieu, Case Courrier 121, 75005 Paris, France*

[2]*Institute of Physical Chemistry, Polish Academy of Sciences, Kasprzaka 44/52, 01-224 Warsaw, Poland*

[3]*Physics Laboratory, Warsaw University of Agriculture, Nowoursynowska 159, 02-776 Warsaw, Poland*

(Received 5 February 2008; revised manuscript received 20 June 2008; published 21 July 2008)

We consider the two classes of exothermic chemical wave fronts, propagating toward a stable or an unstable steady state. The hydrodynamic equations for stream velocity, temperature, and concentrations are solved numerically for increasing values of the reaction heat. For a critical value of the heat release, we find a transition between a chemical front, whose speed depends on the chemical dynamics, and a generic flame, whose speed is entirely determined by heat release. We derive an analytical expression of the flame speed from the invariants of the hydrodynamic equations. This result substantiates macroscopic approaches widely used in combustion, in which the chemical models include only simplified reaction mechanisms.

DOI: 10.1103/PhysRevE.78.016309 PACS number(s): 47.70.Fw, 47.70.Pq, 82.40.Ck

I. INTRODUCTION

Chemical wave fronts are concentration waves that propagate without deformation and replace a steady state by another one. While flame propagation is a basic issue of combustion [1–3], reaction-diffusion fronts are intensively studied in the context of chemical [4–7] and biological [8] systems. There is increasing experimental evidence to suggest that the early stages of many eukaryotic organisms are regulated by the propagation of a chemical wave [9,10]. The so-called clock and wave-front model is now well admitted for vertebrate morphogenesis [11,12]. Heat-inducible misexpression during fish embryogenesis has been recently exhibited [10]. In this paper, we revisit the problem of front propagation speed selection in the case of exothermic reactions. To make the link between combustion and reaction-diffusion processes, we study how the propagation speed of an exothermic front varies with increasing heat release. Our goal is to determine if exothermicity induces a small perturbation or if it qualitatively changes the properties of the traveling front. To check the universality of the phenomenon, we consider the two kinds of reaction-diffusion fronts, propagating either toward an unstable steady state or between two stable steady states. The Fisher [13] and Kolmogorov-Petrovsky-Piskunov model [14],

$$A + B \xrightarrow{k} 2A + \text{heat } Q \tag{1}$$

introduced for $Q=0$ to describe the propagation of an advantageous gene into a population, serves as the reference model of autocatalytic reactions with a quadratic dynamics. It is used to analyze the isothermal reaction fronts that replace an unstable steady state a_0 by a stable steady state a_{st}. The modified Schlögl model [15,16], which is associated with a cubic dynamics,

$$2A + B \xrightarrow{k_1} 3A + \text{heat } Q, \tag{2}$$

$$A \xrightarrow{k_2} B - \text{heat } Q, \tag{3}$$

is a minimal model exhibiting, for $Q=0$, two stable steady states, (a_{st}, a_0), for appropriate rate constants k_1 and k_2. For these simple, generic models, the analytical expression of the front propagation speeds is known in the case of isothermal reactions and the results of the macroscopic reaction-diffusion equations have been confirmed by simulations at the microscopic level [7,16–19]. We recently studied exothermic Fisher fronts in the frame of a macroscopic description [20] and solved numerically the hydrodynamic equations for increasing values of the activation energy of the reaction. We proved the existence of a forbidden propagation speed interval, where the system does not admit steady traveling solutions. Qualitatively, the reactive interface can be seen as a traveling heat source, generating forward and backward heat fronts. In the forbidden domain, the forward heat front would propagate at a speed close to that of the reaction interface, so that the distance between these two interfaces would always remain constant. In these conditions, the heat released by the reaction accumulates in the vicinity of the reactive interface and this sustained thermal perturbation prevents reaching steady traveling interfaces.

The paper is organized as follows. In Sec. II, we write the hydrodynamic equations associated with the Fisher model and the Schlögl model. We use the expressions of the transport coefficients which are valid for a dilute gas, in order to make possible a comparison with microscopic simulations. The results of the numerical integration of these equations are given in Sec. III. A qualitatively different behavior is found as the heat release exceeds a critical threshold. After the transition, we show that the flame has a universal behavior, in the sense where its speed does not depend on the chemical model and on the activation energies. The propagation speeds of the exothermic chemical fronts deduced from the numerical solutions are compared with analytical predictions. We propose in the Conclusion an experimental system that could be used to validate the theoretical results.

*Author to whom correspondence should be addressed. anle@lptmc.jussieu.fr

II. THE BALANCE EQUATIONS OF THE THERMOCHEMICAL SYSTEM

For each model of exothermic chemical fronts, the dynamics is governed by the following balance equations [27] for total concentration $\rho(x,t)$, stream velocity $u(x,t)$, temperature $T(x,t)$, and concentration $a(x,t)$ of species A:

$$\partial_t \rho = -\partial_x(\rho u), \tag{4}$$

$$\partial_t u = -\frac{1}{m\rho}\partial_x\left(k_B\rho T - \frac{4}{3}\eta_0\sqrt{T}\partial_x u\right) - u\partial_x u, \tag{5}$$

$$\partial_t T = \frac{T}{3}\partial_x u + \frac{8\eta_0\sqrt{T}}{9k_B\rho}(\partial_x u)^2 - \partial_x(uT) + \frac{f_0}{k_B\rho}\partial_x(\sqrt{T}\partial_x T) + \frac{2QR}{3k_B\rho}, \tag{6}$$

$$\partial_t a = -\partial_x(au) + d_0\partial_x[\sqrt{T}\partial_x(a/\rho)] + R, \tag{7}$$

where the fluid is assumed to obey the ideal-gas law and where the reactive term R is given by $R_F=ka(\rho-a)$ for the Fisher model and by $R_S=k_1a^2(\rho-a)-k_2a$ for the Schlögl model. In the absence of reaction, the reactive term vanishes and Eqs. (4)–(6) reduce to the Navier-Stokes equations for a dilute inert gas [28], i.e., to the conservation equations for mass, momentum, and energy. The macroscopic description can be readily extended to any fluid, but we apply it to a dilute gas to make possible a comparison with microscopic simulations based on the direct simulation Monte Carlo method [21], which is valid for low-density gases [22,23]. The extension to solid flame is not straightforward. The mechanisms governing self-propagating high-temperature synthesis (SHS) [24] have the complexity of multiphase reactions, such as dissolution-precipitation and heterogeneous nucleation processes that are not included in this description. Moreover, solid combustion should take into account the existence of stresses induced by the exothermic processes.

The reservoirs of species C of the original Schlögl model [15], $C+2A \rightleftharpoons 3A$, $A \rightleftharpoons C$, are difficult to simulate at the microscopic level. Previously [16], we introduced the modified model given in Eqs. (2) and (3) in order to avoid resorting to tanks. The choice of a molecular model and an interaction potential makes it possible to use explicit expressions for the transport coefficients. For the hard-sphere model [21,29], the heat conductivity reads $f_0\sqrt{T}=\frac{25k_B}{32\sigma}\sqrt{\frac{\pi k_B T}{m}}$ for particles of cross section σ and mass m, the diffusion coefficient is $d=d_0\sqrt{T}/\rho$ with $d_0=\frac{3}{8\sigma}\sqrt{\frac{\pi k_B}{m}}$, and the shear viscosity is $\eta_0\sqrt{T}=\frac{5}{12\sigma}\sqrt{\pi k_B T m}$. According to kinetic theory for reactive hard spheres [21], the rate constant of the Fisher model is $k=4\sigma\sqrt{\frac{k_BT}{\pi m}}\exp(-\frac{E_a}{k_BT})$, where E_a is the activation energy of the autocatalytic reaction. The introduction of processes with simultaneous interaction of three particles poses a problem in the hard-sphere model. To mimic three-body collisions, we use a solution introduced in microscopic simulations of the Brusselator model [25], which we already adapted to the modified Schlögl model [16]: a three-molecular collision is seen as a binary collision with a third molecule in the nearest neighborhood of the colliding pair. The rate constant $k_1=k/\rho$ of the ternary collisions (A, A, B) is deduced from the expression that is obtained for binary collisions (A, B) that is corrected by the concentration of species A.

We consider the stationary reaction fronts, $a(x,t)=a(x-Ut)$, moving at speed U in the positive direction of the x axis. The invariants deduced from Eqs. (4)–(7) lead to Hugoniot relations [26,27] between the values of the hydrodynamic variables ahead of (index 1) and behind (index 2) the front [20],

$$\rho_2(u_2-U) = \rho_1(u_1-U), \tag{8}$$

$$k_B\rho_2T_2 + m\rho_2(u_2-U)^2 = k_B\rho_1T_1 + m\rho_1(u_1-U)^2, \tag{9}$$

$$\frac{5}{2}k_BT_2 + \frac{m}{2}(u_2-U)^2 = \frac{5}{2}k_BT_1 + \frac{m}{2}(u_1-U)^2 + Q. \tag{10}$$

The step (u_2-u_1) of stream velocity obeys a second-order polynomial equation that does not admit real roots if $U \in]U_-, U_+[$, where

$$U_\pm = u_1 + \sqrt{\frac{15T_1k_B + 16Q \pm 4\sqrt{2Q(15T_1k_B+8Q)}}{9m}}. \tag{11}$$

For both models, we start from a uniform condition for total concentration ρ_0, stream velocity $u_0=0$, temperature T_0, and from a step function for the concentration of species A with $a(x,t)=a_{st}$ for $x\leqslant 0$ and $a(x,t)=a_0$ for $x>0$, where a_{st} and a_0 are steady states for $Q=0$. The reaction fronts of these two models propagate toward $a_0=0$, in which the reactions are stopped due to the lack of species A. A microscopic approach requires that a_0 is not sensitive to fluctuations of concentrations that would induce spontaneous transitions toward a_{st} before the passage of the front. For the Schlögl model, the irreversibility of the second reaction ensures the existence of $a_0=0$. In the Fisher model, one has $a_{st}=\rho_0$, and in the Schlögl model, $a_{st}=\frac{\rho_0}{2}(1+\sqrt{1-\frac{4k_2}{k_1\rho_0^2}})$ for parameters such that the square root is defined and where k_1 is evaluated in isothermal conditions.

We solve numerically Eqs. (4)–(7) using the Euler method [20]. Due to the propagation of the reactive interface $a(x-Ut)$ and to the forward and backward heat fronts, we must increase the length L of the medium during the computation. We continuously check the values of the hydrodynamic variables ρ, u, and T in cells 50 and $L-50$. As soon as the value of one of these variables differs, at the computing precision, from the initial value ρ_0, u_0, or T_0, we extend the system by one cell at the corresponding boundary. Hence, we keep an unperturbed boundary layer of 50 cells at each extremity of the medium during the whole computation. We choose initial temperature $k_BT_0=1$, particle mass $m=1$, time step $\Delta t=10^{-2}$, spatial discretization into cells of length $\Delta L=1$ unless otherwise stated, cross section $\sigma_F=0.0794$ and initial total concentration $\rho_{0F}=20$ for the Fisher model, $\sigma_S=0.001$, $\rho_{0S}=40$, and rate constant $k_2=0.001$ for the Schlögl model.

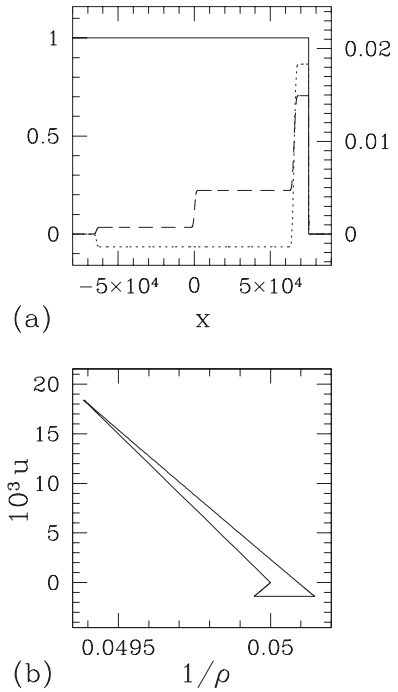

FIG. 1. Fisher model: Numerical solution of Eqs. (4)–(7) for activation energy $E_a=1$ and heat release $Q=0.01$ after 5×10^6 integration time steps. (a) Left axis: scaled concentration profile a/ρ of species A (solid line). Right axis: temperature shift $T-T_0$ (dashed line) and stream velocity u (dotted line). (b) Stream velocity u vs reciprocal of total concentration $1/\rho$.

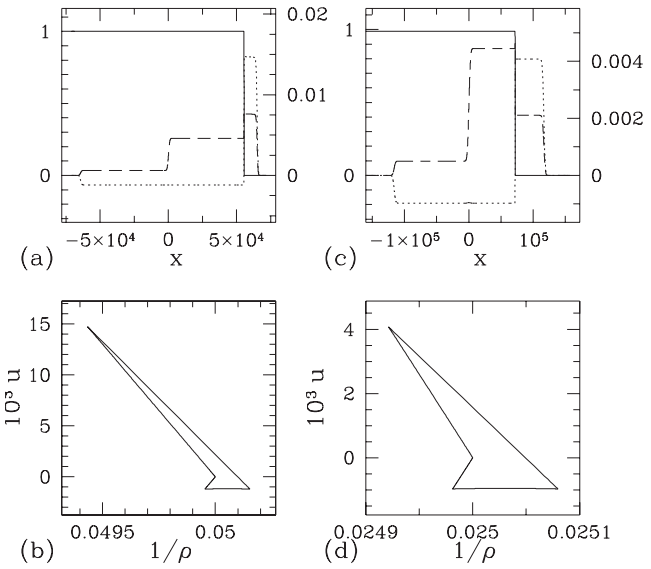

FIG. 2. (a) and (b) Same caption as Fig. 1 for the Fisher model with $E_a=1.65$ and $Q=0.01$. (c) and (d) Same caption as Fig. 1 for the Schlögl model with $E_a=0.1$ and $Q=0.01$ after 9×10^6 integration time steps.

III. RESULTS

In the isothermal case $Q=0$, the hydrodynamic variables are constant. The speed U of the reaction front is obtained from solutions of the reaction-diffusion equation given in Eq. (7) for $u=0$, $\rho=\rho_0$, $T=T_0$. For the Fisher model [7], one has $U_F=2\sqrt{k\rho_0 d}$. Depending on the activation energy E_a, the speed U_F can be larger (small E_a) or smaller (large E_a) than the sound speed $U_{\text{sound}}=\sqrt{\frac{5k_BT_0}{3m}}$ at temperature T_0. For the isothermal Schlögl model [16], the speed is given by $U_S=\frac{\rho_0}{2}\sqrt{\frac{k_1 d}{2}}\left(3\sqrt{1-\frac{4k_2}{k_1\rho_0^2}}-1\right)$. The largest value, $\frac{1}{2}\sqrt{\frac{3k_BT_0}{m}}$, obtained for $(E_a\to0,\ k_2\to0)$, is smaller than the sound speed.

For small values of heat release Q, two qualitatively different behaviors are observed for the Fisher model and only one for the Schlögl model.

Figure 1(a) gives the results of the numerical integration of Eqs. (4)–(7) for the Fisher model. It represents the profiles for scaled concentration a/ρ, temperature deviation $(T-T_0)$, and stream velocity u for a small value of the activation energy. In this case, the reactive front is the first step encountered from the right boundary. The second step and the fourth step are the forward and backward heat fronts, propagating, respectively, to the right and to the left. The third interface close to $x=0$ is reminiscent of the initial condition. We give in Fig. 1(b) a diagram that represents stream velocity u versus $1/\rho$. According to mass conservation, already used to derive the first Hugoniot relation given in Eq. (8), we have $u=-\rho_0 U/\rho+U$. The relation applies for any kind of stationary waves traveling at speed U. The straight lines observed in Fig. 1(b) prove that the four interfaces are stationary traveling fronts. The y intercept gives the propagation speed. The straight line with the largest (in absolute value) negative slope is associated with the fastest front, here the reaction front. The other line with a negative slope corresponds to the forward heat front, propagating slower than the reactive front, at a speed close to the sound speed. The nearly horizontal line is related to the reminiscence of the initial condition; it moves very slowly to the left. Finally, the segment with a positive slope is associated with the backward heat front. Such a behavior, where the reaction front propagates faster than the forward heat front, cannot be observed in the case of the Schlögl model.

For a larger activation energy and still a small heat release, another type of behavior is obtained for both models, as given in Fig. 2. Now, the first interface from the right is the forward heat front. It propagates faster than the reaction front. The four interfaces are stationary wave fronts, as shown by the straight lines in the $(1/\rho,u)$ diagram given Figs. 2(b) and 2(d).

For each model, we performed series of calculations for several fixed values of activation energy E_a and variable heat release Q. Figure 3 shows how the propagation speed U of the reaction front varies with Q. The solid lines represent the two critical speeds, U_- and U_+, which limit the forbidden domain of propagation speed [20]. They have been deduced from Eq. (11) in which the temperature T_1 and the stream velocity u_1 ahead of the reaction front are assumed to be unperturbed, i.e., $T_1=T_0$ and $u_1=0$. The dashed line corresponds to the sound speed at temperature T_0.

For the Fisher model and the first series at a small activation energy $E_a=0.8$, the reaction front is the fastest interface that propagates toward the unperturbed medium at T_0. The profiles given in Fig. 1 illustrate this case. The speed of pulled fronts [30], propagating toward an unstable state such

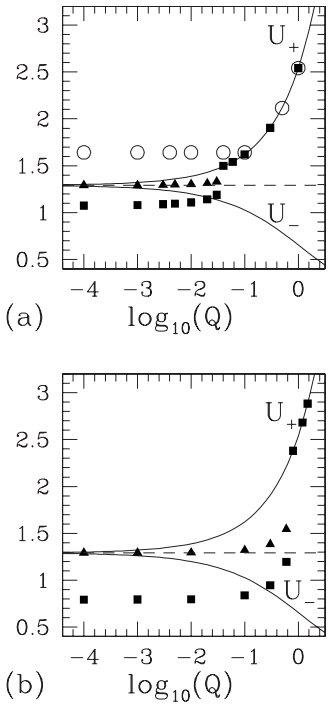

FIG. 3. Critical reaction front speeds U_- and U_+ given in Eq. (11) vs $\log_{10}(Q)$ (solid lines), sound speed at T_0 (dashed line), and heat front speed propagating to the right (solid triangles). (a) Fisher model: reaction front speed given by the numerical solutions of Eqs. (4)–(7) for $E_a=0.8$ (open circles) and $E_a=1.65$ (solid squares). (b) Schlögl model: reaction front speed for $E_a=0.1$ (solid squares).

as Fisher front, is determined by the leading edge. As shown in Fig. 3(a), the speeds U that are greater than U_+ are given by the unperturbed expression $U=2\sqrt{k\rho_0 d}$, as in the isothermal case. The open circles, associated with a small value of activation energy E_a, are on a horizontal line for sufficiently small values of heat release Q. For a critical heat release, this horizontal line intersects the upper branch U_+. As Q is increased further, the reaction front speed follows the upper branch U_+.

For the Fisher model and the second series at a higher activation energy $E_a=1.65$ and still small heat releases, the reaction front is preceded by the heat front. Figure 2 gives a typical example of this behavior. The leading edge of the reaction front is therefore perturbed by the temperature increase behind the heat front and the propagation speed U of the reaction front is slightly larger than in the isothermal case. As shown in Fig. 3(a), the solid squares are on a slowly increasing curve until this curve slightly exceeds the lower branch U_-. Then, an abrupt transition is observed as Q increases and the speed remains attached to the upper branch U_+, exactly as in the previous series at $E_a=0.8$. The critical value of Q at which the transition occurs depends on activation energy E_a. After the transition, the propagation speed, fixed at U_+, is determined by Q only. It does not depend on the activation energy.

For the Schlögl model, the reaction front is always behind the forward heat front and the reaction front speed is perturbed with respect to the isothermal case. As seen in Fig. 3(b), the transition is smoother than for the Fisher model and

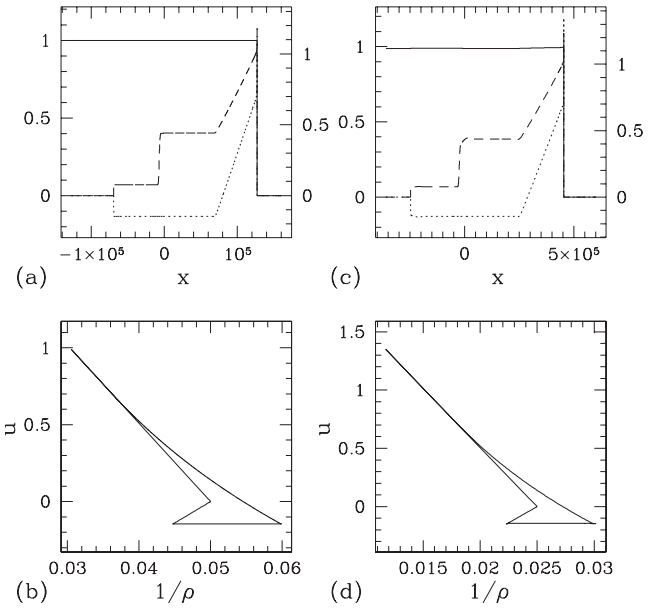

FIG. 4. (a) and (b) Same caption as Fig. 2 for the Fisher model with $E_a=1$ and $Q=1$ after 5×10^6 integration time steps. (c) and (d) Same caption as Fig. 2 for the Schlögl model with $E_a=0.1$ and $Q=1$ after 18×10^6 integration time steps and a cell length $\Delta L=6$.

occurs after the lower branch, U_-, has been crossed. A larger temperature increase, ahead of the reactive interface, is necessary to destabilize a pushed reaction front, whose speed depends on the entire profile and not only on the leading edge [16].

The main result is that, after the transition, the propagation speed at a given Q corresponds to the value of U_+ for this heat release, for the Schlögl model as well as for the Fisher model. The propagation speed is then entirely determined by Q and does not depend on the specific nonlinearities of the chemical model. The same property applies to the profiles of the hydrodynamic variables, as seen in Figs. 4(a) and 4(c). According to Figs. 4(b) and 4(d), only three segments of the $(1/\rho,u)$ diagram are straight lines: only three stationary traveling fronts are observed and the forward heat front is replaced by a continuously stretching interface behind the reaction front. The speed U_+ on the critical upper branch can be calculated exactly from the analytical expression given in Eq. (11), since the relations $T_1=T_0$ and $u_1=0$ are rigorously satisfied on this branch.

IV. CONCLUSION

We have performed a hydrodynamic description of a reactive flow that possesses an exothermic traveling front. For the sake of generality, we consider two minimal chemical models, which cover the description of the two types of chemical wave fronts, that travel either toward a stable stationary state or an unstable one. For a sufficiently small heat release Q, an exothermic reaction wave front is either faster or slower than the forward heat front. For such small heat releases, the propagation speed of the reaction front and the profiles of the hydrodynamic variables depend on the chemi-

cal model and on the activation energy. We have shown that a transition occurs for a value of heat release that depends on the model and on the dynamical parameters. After the transition, we observe a generic flame, independent of the chemical model and of its parameters, whose properties are entirely determined by heat release Q. These results rely on the existence of a forbidden interval for stationary front speed, which has been derived on the basis of the hydrodynamic invariants. We give an analytical expression for the two branches, U_- and U_+, which limit the domain of forbidden speeds for stationary fronts. Qualitatively, the forbidden domain corresponds to parameters for which the heat front and the reaction interface propagate at the same speed, so that heat accumulates at the level of the reaction interface and destabilizes it. The transition between a model-dependent front and a generic flame occurs when the propagation speed of the reaction front reaches one of the boundaries of the forbidden domain. After the transition, the system selects the marginally stable solution associated with the smallest permitted propagation speed, compatible with an increase with Q, i.e., the critical upper branch U_+ of the forbidden domain.

These results give credit to macroscopic approaches widely used in combustion [31,32] in which the chemical models include only very simplified reaction mechanisms. We show that, when the heat release is sufficiently large, the nonlinearities induced by the specific concentration dependence of the chemical model and even the value of the activation energies do not influence the flame properties.

We have solved the hydrodynamic equations in the case of a dilute gas in order to be able to compare the macroscopic predictions with microscopic simulations of particle dynamics. We intend to use the direct simulation Monte Carlo method, which was already implemented for reactive flows and that requires the dilute gas assumption. The invariants and consequently the two branches, U_- and U_+, do not involve any transport coefficient or chemical rate constant. Their expression only uses the usual ideal-gas assumption, which neglects particle interaction contribution to energy and pressure. Therefore, we can expect that the existence of a transition and the value of the flame speed after the transition are not related to any specific property of the systems we considered. The rather generic character of our results suggests that they remain valid for any fluid.

The skeletal isomerization of butene over well-chosen pore size zeolites [33] could be a good candidate for an experimental validation. For medium pore size zeolites, the transformation of *n*-butene into isobutene is known to follow a bimolecular, autocatalytic mechanism, and a wave front of Fisher type could be observed in a long cylindrical reactor prepared with *n*-butene and isobutene at equilibrium on the left and isobutene on the right. A wave front of Schlögl type can be envisaged for larger pore size zeolites, which favor trimolecular reactions. The heat release can be varied by using derivatives of butene resulting from the substitution of a hydrogen by different functional groups. According to our results, possible changes of mechanism and activation energy should not affect the flame speed after the transition. The experimental determination of the flame propagation speed for different derivatives could be used to check if the marginally stable speed associated with the upper branch of the forbidden domain is actually selected.

ACKNOWLEDGMENTS

The authors acknowledge financial support from the joint project 20146 between CNRS (France) and PAN (Poland). M.L. acknowledges CNRS for support.

[1] V. Bychkov, A. Petchenko, V. Akkerman, and L. E. Eriksson, Phys. Rev. E **72**, 046307 (2005).
[2] S. Kadowaki, H. Suzuki, and H. Kobayashi, Proc. Combust. Inst. **30**, 169 (2005).
[3] M. Matalon, Annu. Rev. Fluid Mech. **39**, 163 (2007).
[4] J. D'Hernoncourt, S. Kalliadasis, and A. De Wit, J. Chem. Phys. **123**, 234503 (2005).
[5] J. D'Hernoncourt, A. De Wit, and A. Zebib, J. Fluid Mech. **576**, 445 (2007).
[6] J. D'Hernoncourt, A. Zebib, and A. De Wit, Chaos **17**, 013109 (2007).
[7] J. S. Hansen, B. Nowakowski, and A. Lemarchand, J. Chem. Phys. **124**, 034503 (2006).
[8] J. D. Murray, *Mathematical Biology. I: An Introduction* (Springer, Berlin, 2002).
[9] D. Dormann, B. Vasiev, and C. J. Weijer, Biophys. Chem. **72**, 21 (1998).
[10] B. Bajoghli, N. Aghaallaei, T. Heimbucher, and T. Czerny, Dev. Biol. **271**, 416 (2004).
[11] R. E. Baker, S. Schnell, and P. K. Maini, J. Math. Biol. **52**, 458 (2006).
[12] M. Kaern, D. G. Miguez, A. P. Munuzuri, and M. Menzinger, Biophys. Chem. **110**, 231 (2004).
[13] R. A. Fisher, Annals Eugen. **7**, 355 (1937).
[14] A. N. Kolmogorov, I. G. Petrovsky, and N. S. Piskunov, Moscow Univ. Math. Bull. **1**, 1 (1937).
[15] F. Schlögl, Z. Phys. **253**, 147 (1972).
[16] A. Lemarchand and B. Nowakowski, Phys. Rev. E **62**, 3156 (2000).
[17] A. Lemarchand and B. Nowakowski, Europhys. Lett. **41**, 455 (1998).
[18] B. Nowakowski and A. Lemarchand, J. Chem. Phys. **109**, 7028 (1998).
[19] A. Lemarchand and B. Nowakowski, J. Chem. Phys. **111**, 6190 (1999).
[20] M. Leda, A. Lemarchand, and B. Nowakowski, Phys. Rev. E **75**, 056304 (2007).
[21] G. A. Bird, *Molecular Gas Dynamics and the Direct Simulation of Gas Flows* (Clarendon, Oxford, 1994).
[22] J. S. Hansen, B. Nowakowski, and A. Lemarchand, J. Chem. Phys. **125**, 044313 (2006).
[23] B. Nowakowski and A. Lemarchand, J. Chem. Phys. **127**, 174712 (2007).
[24] A. Lemarchand and J. P. Bonnet, J. Phys. Chem. C **111**, 10829

(2007).
[25] M. Mareschal and A. De Wit, J. Chem. Phys. **96**, 2000 (1992).
[26] Y. B. Zel'dovich and Y. P. Raizer, *Physics of Shock Waves and High-Temperature Hydrodynamics Phenomena* (Academic, New York, 1966).
[27] E. Salomons and M. Mareschal, Phys. Rev. Lett. **69**, 269 (1992).
[28] B. L. Holian, C. W. Patterson, M. Mareschal, and E. Salomons, Phys. Rev. E **47**, R24 (1993).
[29] D. A. McQuarrie, *Statistical Mechanics* (Harper and Row, New York, 1973).
[30] E. Brunet and B. Derrida, Phys. Rev. E **56**, 2597 (1997).
[31] D. A. Frank-Kamenetskii, *Diffusion and Heat Exchange in Chemical Kinetics* (Princeton University Press, Princeton, NJ, 1955).
[32] Y. B. Zeldovich, G. I. Barenblatt, V. B. Librovich, and G. M. Makhviladze, *The Mathematical Theory of Combustion and Explosions* (Plenum, New York, 1985).
[33] M. Guisnet, P. Andy, N. S. Gnep, E. Benazzi, and C. Travers, Oil Gas Sci. Technol. **54**, 23 (1999).